Brazilian Journal of Geophysics, **42** (2024), 3, 1–11
Brazilian Geophysical Society
ISSN 2764-8044
DOI 10.22564/brjg.v42i3.2326

PORE TYPE AND ASPECT RATIO PREDICTION – A KNOWN PARAMETER FOR SEISMIC MONITORING STRATEGIES – AND THE APPLICATION ON PRE-SALT RESERVOIR CARBONATE ROCKS

Evângela P.A. da Silva [1*], Alessandra Davolio [2], Marcos S. dos Santos [2], and Denis J. Schiozer [2]

[1]Petrobras, Santos, SP, Brazil
[2]Universidade Estadual de Campinas - Unicamp, CEPETRO, Campinas, SP, Brazil

*Corresponding author: evangela@petrobras.com.br

ABSTRACT. Microbialites and coquinas compose the large pre-salt carbonate reservoirs for hydrocarbon accumulations of the Santos Basin, Brazilian offshore. The complexity of this type of rock poses major challenges for the reservoir characterization, especially the microbialites. This article presents a well log study relating the deviations of P-wave velocities with the aspect ratio observed in these specific rocks. In our suggested approach, we analyze the facies logs to obtain a relation between these deviation effects and the pore type. The facies analysis allows us to better separate the microbialite and coquina rocks, covering significant differences in porosity and diagenetic processes. We state for the analyzed rocks that the vug features are the predominant pore type for both lithologies, and that this aspect reflects the results of velocity deviations and aspect ratio values. This information is applied to build petroelastic modeling to assist in seismic monitoring of the reservoir.

Keywords: P-wave velocity deviations; petroelastic model; pore type.

INTRODUCTION

Currently, the pre-salt reservoir in the Santos Basin plays as one of the major global exploration and production targets of the last decade. The increasing of systematic study related to this reservoir happens after the conclusion of the first well focusing on that objective (Well 1-BRSA-329D-RJS, called Parati prospect in Block BM-S-10, concluded in 2005). Even not being a commercial well, it has spurred oil and gas exploration until the Tupi discovery, which started its production in 2009 (Maul et al., 2021). Since then, several new fields were discovered in the Santos Basin, and the producing rock formation are Barra Velha and Itapema formations. Microbiolites and coquinas are the main carbonate facies found in these formations (Moreira et al., 2007).

The construction of the petroelastic models requires knowledge of the properties of the pore structure of the rocks, which mainly depend on the morphology pore space and solid phases of rock. The modeling of carbonate reservoirs is more complex than that of siliciclastic ones, due to their distinctions, such as mineralogical composition, environment depositional aspect, diagenetic processes, internal porous structure. Methodologies efficient in the siliciclastic rocks most of the time have deficientness for carbonate rocks, as the siliciclastic ones have mostly ellipsoidal pores (intergranular), the carbonates have pores ranging from rounded and ellipsoidal to elongated. Therefore, the porous geometry has strong influence on carbonate rock physics, imposing important variation for the intrinsically porosity (Mavko et al., 2009).

Choquette and Pray (1970) divide pore type in carbonate rocks into 15 classes, following different aspects of genetics or physics. Because these pore complexities are controlled by diagenetic processes and they give clues about permeability, the pore structure prediction can give us very insightful information about the reservoir characteristic (Harahap et al., 2020).

According to Saberi (2013), the science of rock physics creates a link between elastic properties (e.g., P-velocity/S-velocity ratio, elastic modulus), reservoir properties (e.g., porosity, saturation, pressure) and reservoir architecture (e.g., lamination and fracture). The pore type complexity in carbonate rocks, previously mentioned, affects the seismic primary velocity up to 40% (Xu and Payne, 2009). This complexity gives implications to crossplot scattering in porosity-velocity relationship for the carbonates.

Anselmetti and Eberli (1993, 1997, 1999) demonstrate that the main variations in the geometry of the pore space in carbonates influence the acoustic velocity, confirming a strong dependence on the combination of porosity factors and pore structures. As per the author conclusions, starting from an initial defined velocity, we can observe that: i) velocity positive deviations (above +500 m/s) indicate high velocities related to the porosity, with intrafossil or moldic pores; ii) moldic porosity would be indicative of intense diagenetic changes, favoring the reprecipitation of minerals and cementation of pores. It is characterized by pores commonly not connected with a dense cemented matrix, indicating low permeabilities; iii) deviations close to zero (±500 m/s or less) indicate low velocities, and porosity types such as interparticle, intercrystalline or microporosity, especially associated with few diagenetic changes. There is a predominance of pores typical of the post-sedimentation process, in which the original grains or micrites are packaged together. The aspect is characterized by pores usually well connected producing high permeability, except when only the microporosity is abundant; and iv) negative deviations (below -500m/s), that can be caused by the presence of fractures and gas, excluding the other factors that can also cause low velocities such as well wall problems.

In this work we applied the method proposed by Anselmetti and Eberli (1993, 1997, 1999) to define the aspect ratio of rock appearance by range of velocity deviations P, which will be included in the model proposed by Xu and Payne (2009).

In this way, using the information of one well that reaches the pre-salt reservoir in the Santos Basin as our material of study, we consider the pore geometry influence on the petroelastic model for carbonate rocks affecting the seismic velocity in a different manner, because we assume that for the same porosity value the velocity can be higher or lower depending on the pore type (Castro and Rocha, 2013; Harahap et al., 2020; Silva et al., 2020).

Analysis of the facies log

To assist in the interpretation of the results that were obtained by applying the method mentioned before, the facies created in the well were used, after the calibration, considering the description of samples sides.

The facies logs corresponding to a combination of lithology, type of pores, porosity and diagenetic process, and their respective proportions are shown in Figures 1, 2, 3 and 4, in which the zones corresponding to microbialite and coquina are identified (adapted from Silva et al., 2017).

In Figure 1, we present the lithological facies log, along with graphs of the percentage of these compositions, in addition to three thin sections exemplifying the main lithological types observed in the log. According to the description of the lithofacies log (Figure 1), the microbialite zone is composed of spherulite (33%), laminite (12%), stromatolite (5%); spherulite/laminate (27%) and laminite/spherulite/stromatolite associations (18%); mudstone (3%) and wackstone (2%), not very representative. The coquina range is basically composed of coquina (95%). Figure 1 shows that microbialite is more heterogeneous than coquina, with a predominance of laminites and spherulites in its lithology.

In Figure 2, the porosity log is placed next to the lithological facies log, and we present the graphs in percentage with the main porosities observed in microbialite and coquina. It is worth mentioning that this is a macroscopic classification of porosity. As shown by the facies log of porosity (Figure 2), the best values are found in the coquina interval, in which we interpret mostly as good (48%) and reduced (30%) porosities, while in most of the microbialite interval, we classify the porosity as closed (74%) or reduced (22%).

In Figure 3, in addition to the facies and porosity logs, we show the diagenetic process log along with graphs emphasizing the predominant type of the two zones, microbialite and coquina. Its analysis shows that the porosity seems to be related to the diagenetic process described in the well. It is possible to observe in the process facies log that the dolomitization was the main diagenetic process in the microbialite with occurrence corresponding to $\tilde{6}5\%$; when dolomitization is associated with silicification, the occurrence corresponds to 27%. Silicification occurs in 8% of the rocks. In 6% of the samples, no process was observed.

In coquina, the main diagenetic process (Figure 3) was recrystallization, which is present in almost the entire range. However, only 6% of the rocks occur in an isolated manner. The highest occurrences correspond to the association of recrystallization with dolomitization (37%); and dolomitization with silicification (35%). When the association is only with silicification, the occurrence has a lower expression (7%).

The dolomitization and silicification processes were described in some portions of the log as corresponding to, respectively, 10% and 1.5% of the occurrence in this interval; when both processes are present, the occurrence corresponds to 3.5%.

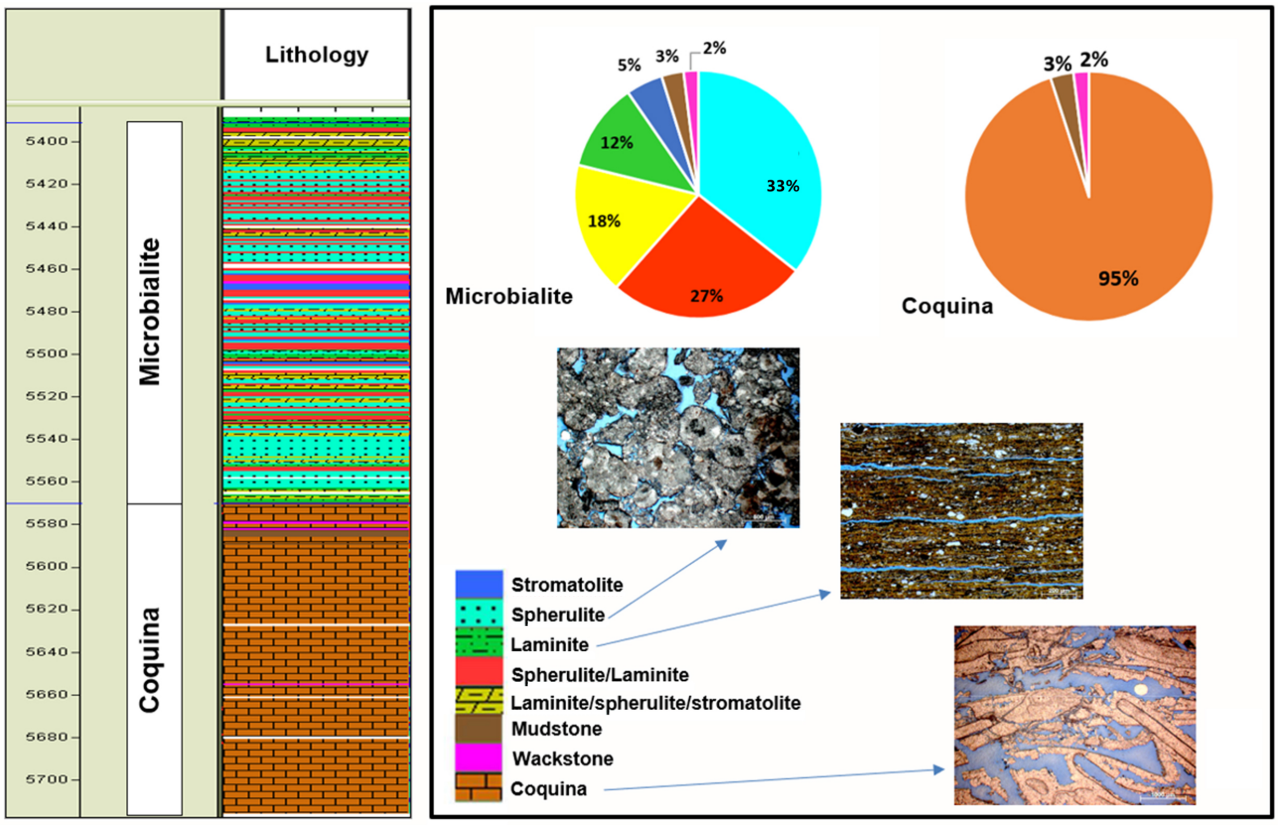

Figure 1: Facies log of lithology showing microbialite and coquina composition in the studied well. Note the predominance of laminite and spherulite in the microbialite. (Adapted from Silva et al., 2017).

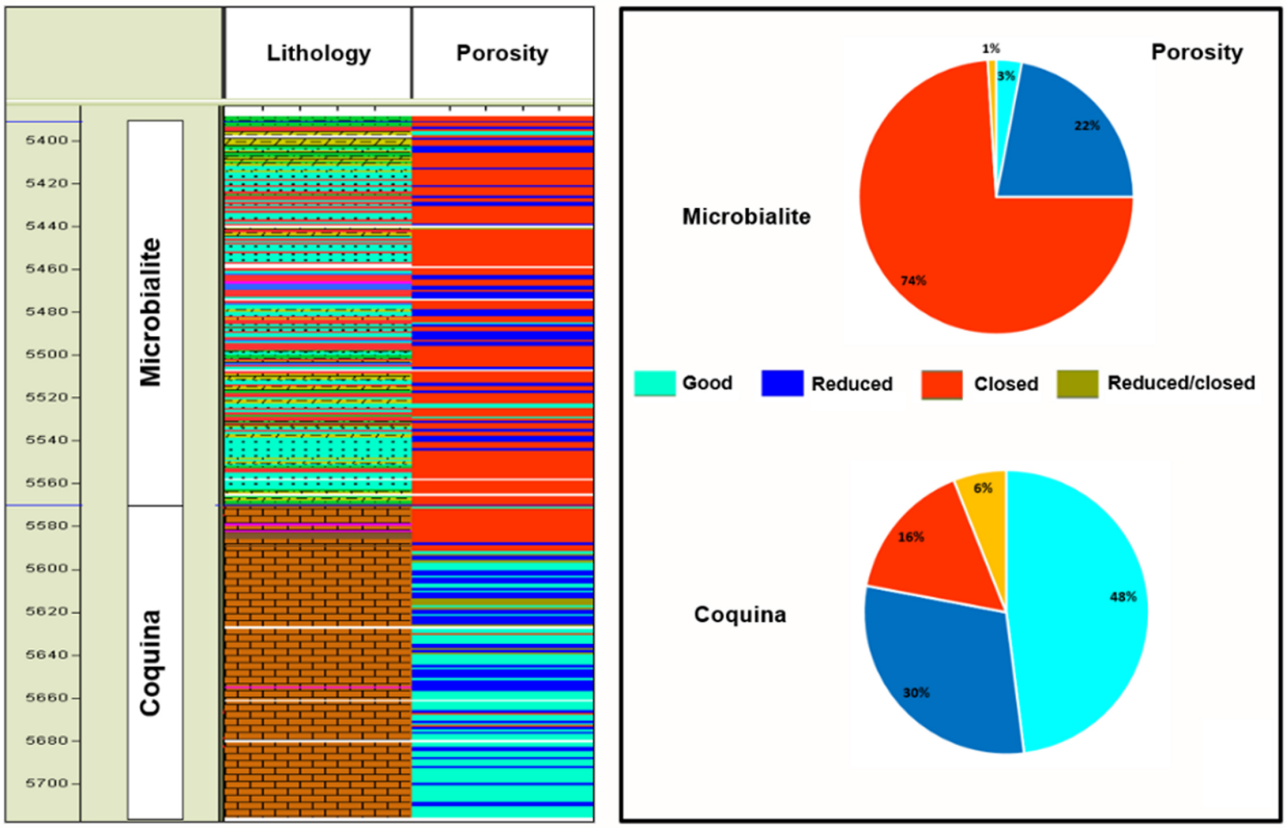

Figure 2: Porosity log next to the facies log. The porosity proportions can be compared between microbialite and coquina, where coquina is observed to be more porous. (Adapted from Silva et al., 2017.)

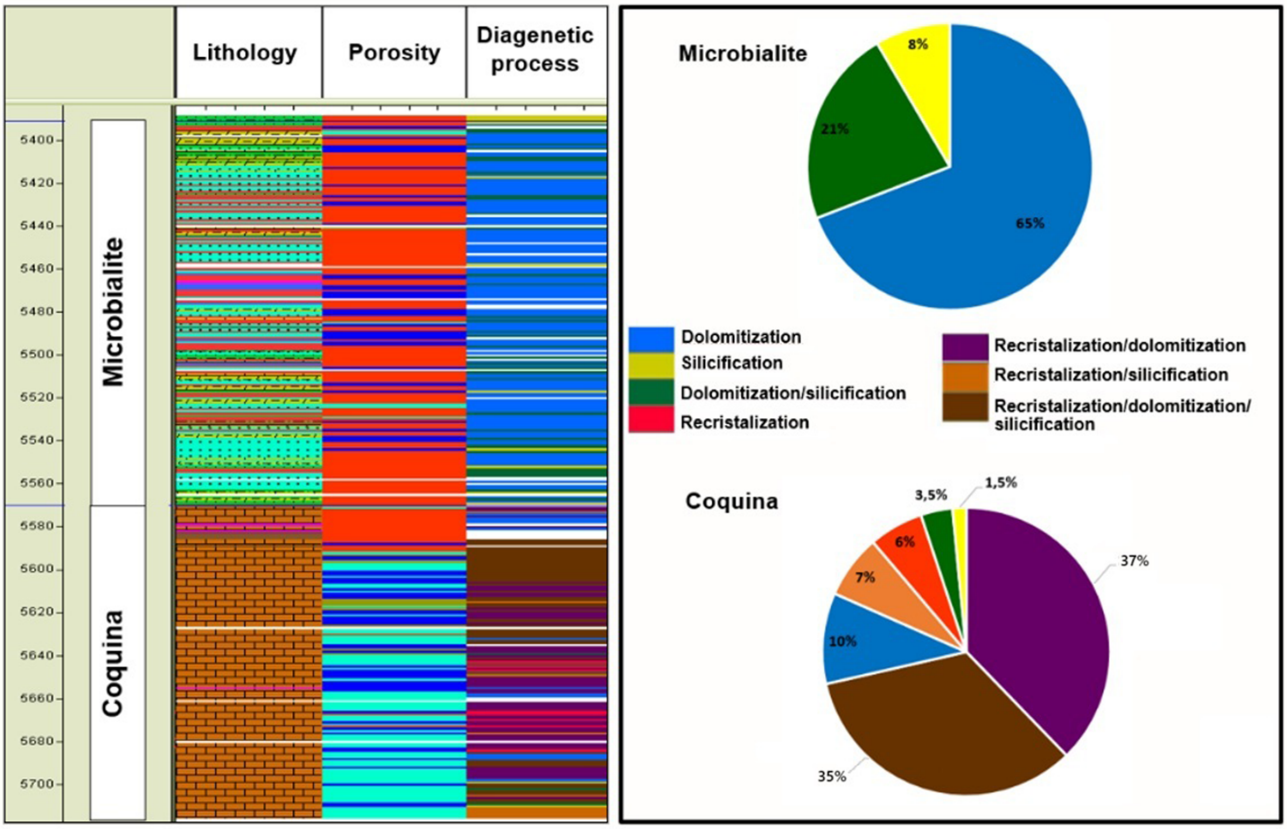

Figure 3: Diagenetic process log next to the facies and porosity logs. It is observed that dolomitization was the dominant process in microbialite, while in coquina it is combined with the recrystallization process. (Adapted from Silva et al., 2017.)

In Figure 4, the pore type log is added to the other ones (lithology, porosity and diagenetic process), together with percentage graphs of their occurrence by zone, and thin sections exemplifying some types of porosity observed in carbonate rocks.

The types of pores we show in Figure 4 emphasize how predominant the vugs are in microbialites, corresponding to approximately 86% of the range; other types of pores also occur in association with vugs (minor occurrences) and they are: framework (6%), fenestral (5%) and intercrystalline (1.3%). When not associated with vugs, the fenestral and framework porosity types represent less than 3% of the range. In coquina, as in microbialite, the predominant type of pores are vugs (45%), which can occur in association with moldic and intercrystalline porosity (31%), or only with moldic (16%) or intercrystalline (6%) porosities. Also, they may be associated with moldic and intergranular (1.5%) porosity. The fenestral porosity corresponds to a 0.5% representation.

The facies analysis performed of the description of lateral samples in the well shows the separation between microbialite and coquina. Given the lithological differences, we analyzed the diagenetic process described in the log samples, in which we observe that the dolomitization, whether or not associated with silicification, predominates in the microbialite facies; while in coquina facies the recrystallization, in association or not with dolomitization and silicification, was the dominant process. In the coquina interval, we noticed the best porosities compared with the microbialite interval occurrences, which often presents closed and/or reduced porosity. Finally, the vug pore type is predominant in both intervals and, in coquina, they are mainly associated with moldic, interparticle and intercrystalline porosity.

GEOLOGICAL SETTING

The Santos Basin is the largest basin along the Brazilian coast, covering an area of about 350.000 km2. As per Garcia et al. (2012), the basin is limited to the NE by the Cabo Frio High and to the South by the Florianopolis High (Figure 5). Its origin begins in the Cretaceous with the breakup of the supercontinent Gondwana, with the opening of the South Atlantic (Kukla et al., 2018) and comprises four unconformity-bounded tectono sedimentary megasequences (Ponte and Asmus, 1978; Chang et al., 1992): the continental rift stage with fluvial and lacustrine sediments dated as Late Jurassic–Early Cretaceous; the Aptian transitional evaporite stage; the Albian restricted marine carbonates; and the open-marine megasequence, dated from the Cenomanian to Present (Moreira et al., 2007).

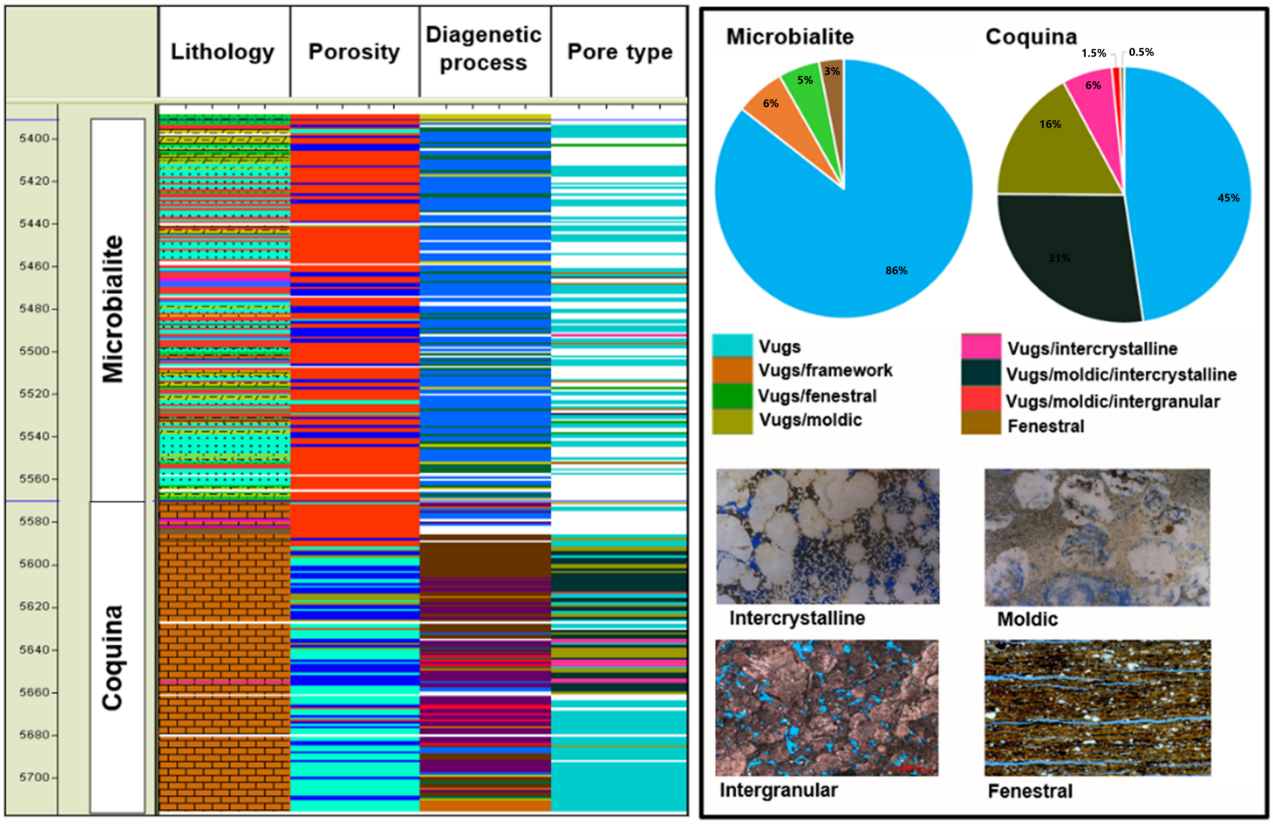

Figure 4: Pore type log next to the facies, porosity, and diagenetic process logs. Note in the pore type proportion graph and in its log that the vug type is predominant in microbialite and coquina. (Adapted from Silva et al., 2017.).

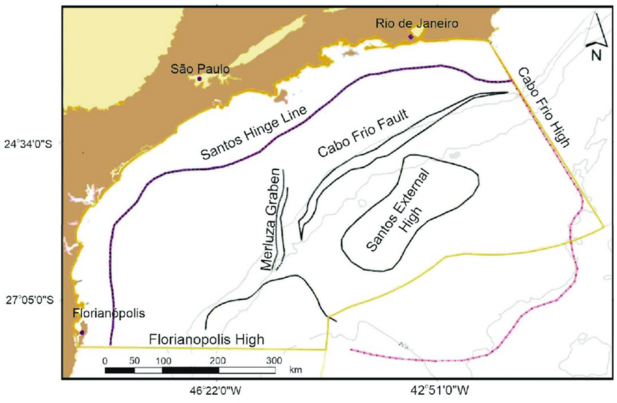

Figure 5: Location and limits of the Santos Basin, Brazilian offshore. (Adapted from Garcia et al., 2012).

The Early Aptian Itapema (ITP) and Barra Velha formations (BVE), which represent the main pre-salt reservoir rocks (Faria et al., 2017), are the subject of this work. They were initially filled by lacustrine to restricted marine carbonates (Mann and Rigg, 2012; Quirk et al., 2012), including coquinas, stromatolites, grainstones, laminites and spherulites. The current stratigraphy adopted for the Santos Basin (Figure 6) generally mentions the rift, transitional (post-rift) and drift phases (Moreira et al., 2007).

Lithostratigraphically, the Itapema Formation is at the top of the sedimentary section of the rift, separated from the Barra Velha Formation by a regional unconformity (pre-Alagoas unconformity), which is at the base of the sedimentary section of the post-rift phase, (Moreira et al., 2007).

The dataset used in this study contains one single well, provided by The Brazilian National Agency of Petroleum, Natural Gas and Biofuels (ANP), and it was chosen because it represents two distinct rock types: microbialite, with main occurrence in the Barra Velha Formation, and coquina, present in the Itapema Formation. The reservoir, with excellent quality oil, is located about 300 km from the Brazilian coast, at total depths of approximately 5,000 meters, with 2,000 meters of water depths, 1,000 meters of mainly siliciclastic sediments and other 2,000 of evaporites (Petrobras website: https://petrobras.com.br/pt/nossas-atividades/principais-operacoes/bacias/bacia-de-santos.htm).

METHODS

To obtain the P-velocity deviation logs, we applied the method proposed by Anselmetti and Eberli (1999), in which new P-wave velocities obtained from the Willie´s equation (Wyllie et al., 1956) are subtracted from the velocity calculated from the sonic

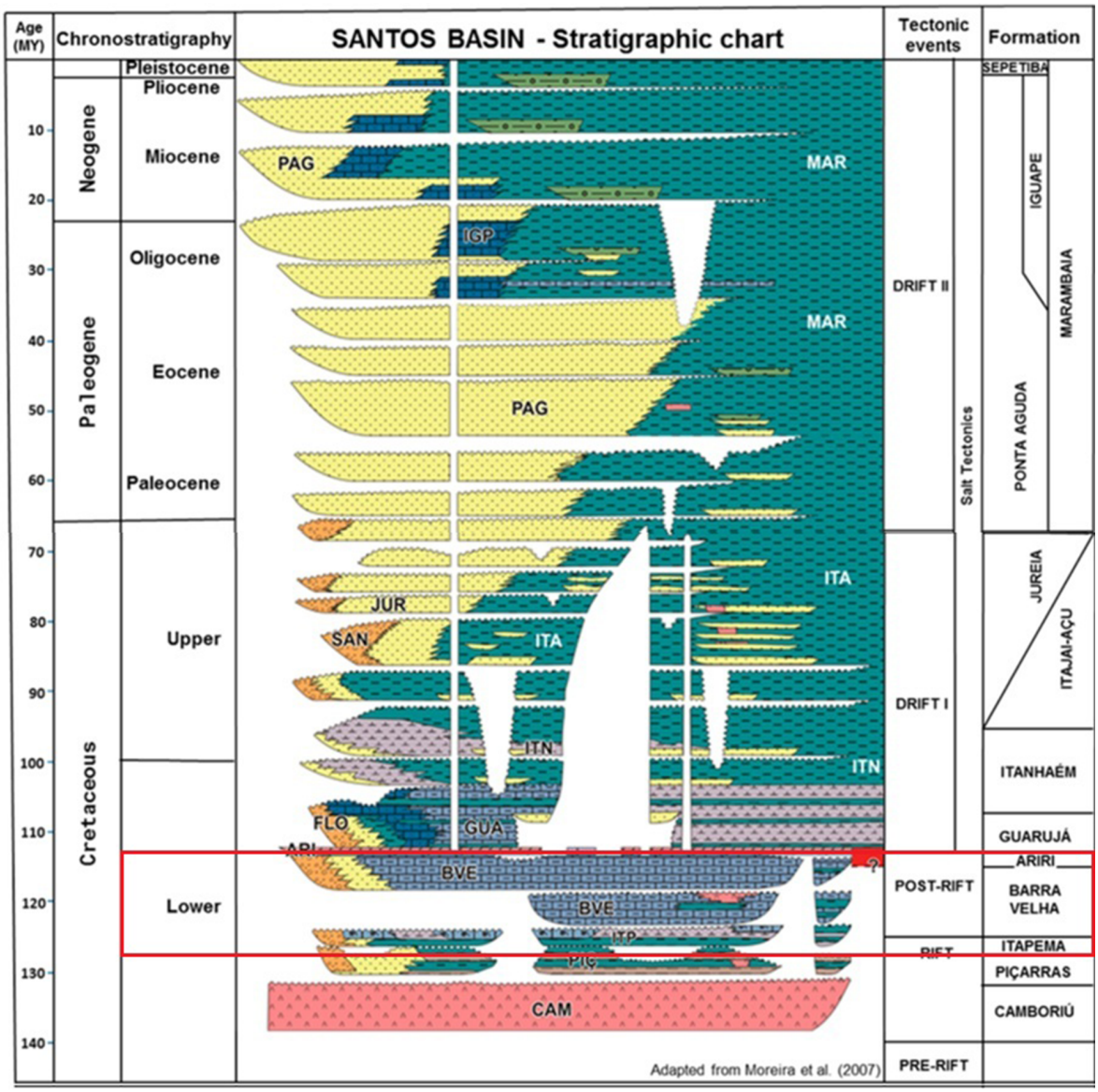

Figure 6: Current Santos Basin stratigraphic chart illustrating the short period of deposition for the Itapema and Barra Velha formations. (Adapted from Moreira et al., 2007).

log. The steps below were carried out:

- Generation of three velocity deviation logs, considering the following input logs of porosity: NPHI (obtained from neutron porosity log), TCMR (obtained from the total porosity of the magnetic resonance log) and Por_RHO (obtained from porosity calculated with the density log);
- Analysis of the three velocity deviation logs to search for patterns allowing us to identify the different areas of interest, and later, to graphically relate such deviations with the aspect ratio of the rock;
- For a better understanding of the results obtained from the P-velocity deviations, we analyzed the logs of lithology, porosity, diagenetic process and pore type, based on the previous interpretation of the sides of the samples ANP provided.

RESULTS, ANALYSIS AND DISCUSSON

Figure 7 shows the results we obtained for the P-wave velocity deviations, based on NPHI, TCMR and Por_RHO, for the microbialite and coquina intervals, along with the water saturation (Sw) and silica volume (V_{si}) logs in the well.

In Figure 8, the results of Pwave velocity deviations were placed next to the lithology, porosity, diagenetic processes and pore type logs, considering only the oil zone in the well. When analyzing the results of deviations from P-velocity (Figures 7 and 8), in terms of positive and negative deviations, it is observed that:

- Deviation from NPHI: microbialite shows a pattern mostly positive and, in contrast, the coquina, in the zone of oil, a pattern predominantly negative. In the water zone of coquina, the deviation pattern intercalates between positive and negative (first part of the log) and neg-

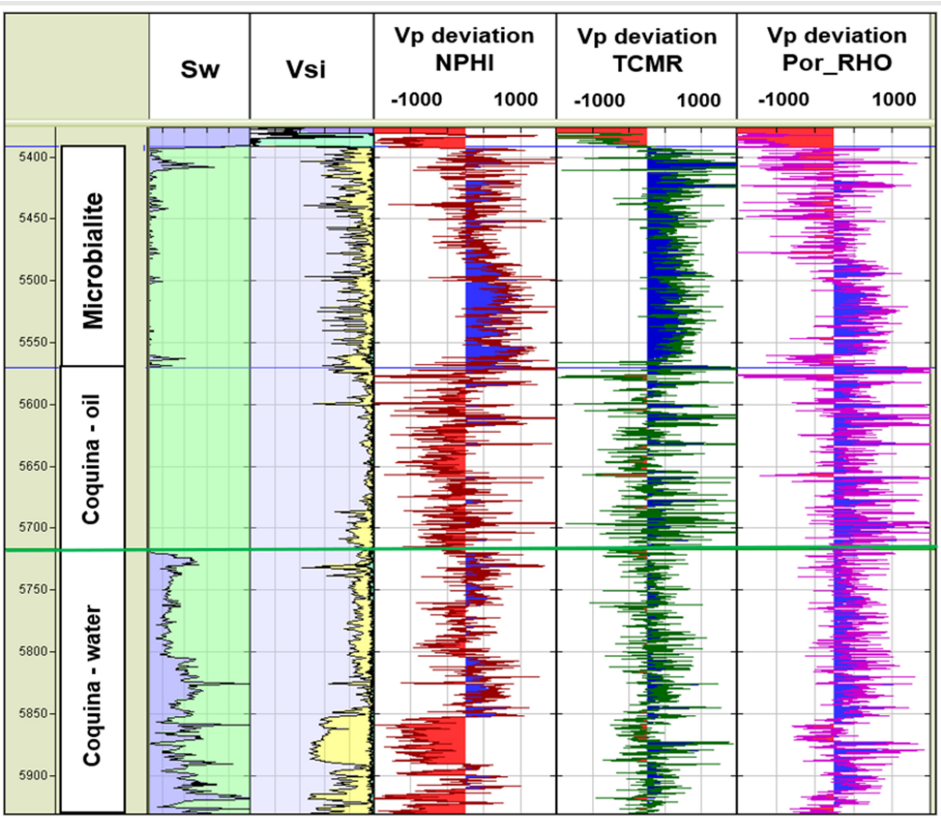

Figure 7: Logs of water saturation (Sw) (in faded blue), silica volume (Vsi) (in yellow) and velocity deviations of the P-wave of the three porosities: NPHI, TCMR and Por_RHO in the microbialite and coquina zones. The positive deviation is shown in blue hatching while the negative deviations are shown in red hatching.

ative (second part), in which the deviations of velocity seem to be influenced by the presence of silica (depth under 5850 m);

- Deviation from TCMR: the deviation pattern in the microbialite is positive, while in coquina it is observed that the deviations oscillate between positive and negative, with predominance of positive values, regardless of the fluid present in the rock (oil or water zone);

- Deviation from Por_RHO: in microbialite, the deviation pattern is both positive and negative, with the first half of the log more negative and the second, positive; in coquina, the pattern is predominantly positive.

Figures 9 and 10 show the P-wave velocity values as a function of porosity, colored by the P-velocity deviation, for microbialite and coquina, respectively. The aspect ratio values present variation between 0.01 and 0.5, in which the higher the value, the more rounded the pore.

The crossplots of Porosity versus Vp (Figures 9 and 10) help to verify the relationship between the velocity deviations and the aspect ratio of rock pores in microbialite and coquina. According to Anselmetti and Eberli (1999), deviation values above 500 m/s are reflections of intrafossil or moldic porosity. In the microbialite zone, it is observed that the vug facies are those that presented such deviation values or, that is, above 500 m/s, which correspond to the aspect ratio above 0.16, regardless of the deviation curve of velocity used. In coquina, it is verified that such deviations are associated with both vugs and moldic porosity, also corresponding to an aspect ratio of 0.16.

Velocity deviations of ±500 m/s (or less) occur due to the presence of interparticle and intercrystalline porosities, according to Anselmetti and Eberli (1999). The results obtained are mostly within their value ranges, where the aspect ratio correspondence is between 0.16 and 0.04, with exception for microbialite in the Por_RHO deviation log and for coquinas in the NPHI deviation log, whose velocity values above −1000 have an aspect ratio of 0.01.

Due to the difference in patterns of velocity deviations obtained in the TCMR log, in which the microbialite was well marked by positive values and the coquina by the oscillation between positive and negative for both oil and water ranges, this log was chosen to define the aspect ratio along the well. Therefore, it is observed that the vuggy and moldic porosities are responsible for the velocity positive deviation, while the interparticle and intercrystalline porosities would be more associated with velocity negative deviations (Figure 8).

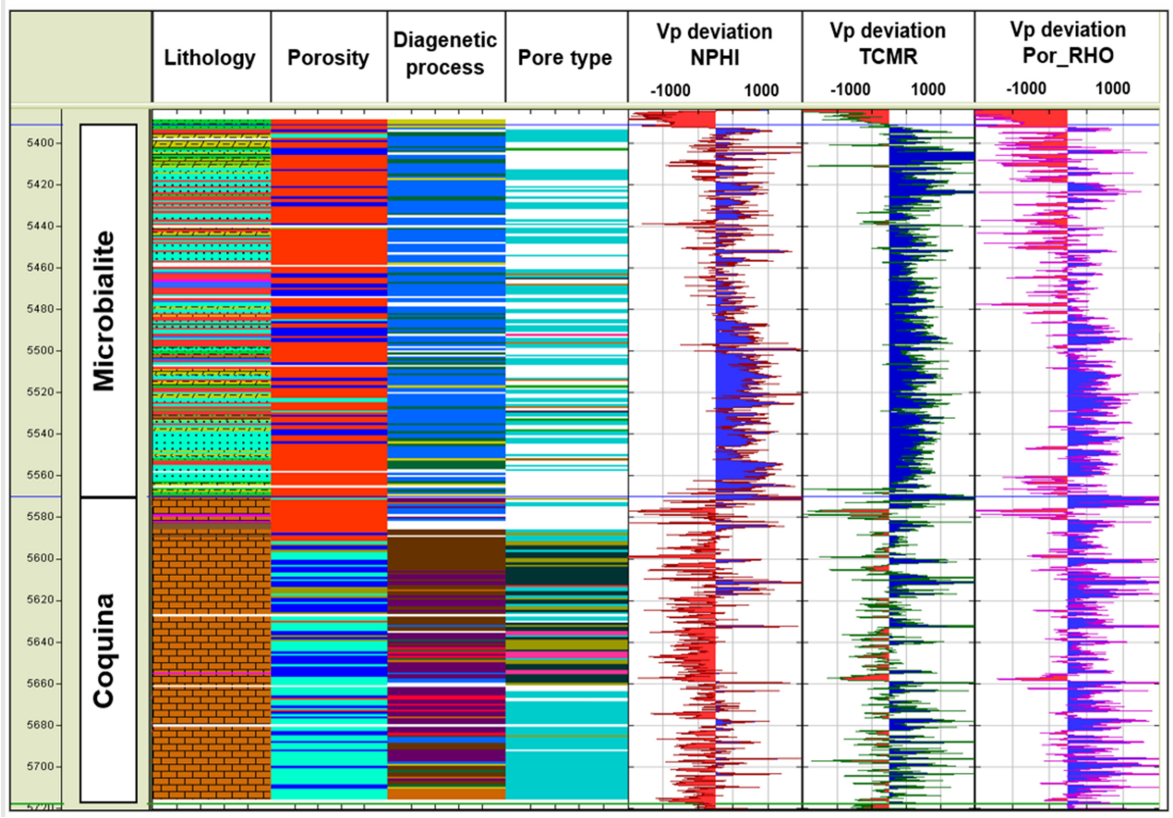

Figure 8: Facies logs - lithology, porosity, diagenetic process and pore type; and deviations of the P-wave velocity of the three porosities: NPHI, TCMR and Por_RHO. The positive deviation is shown in blue hatching while the negative deviations are shown in red hatching.

Table 1: Aspect ratio and its proportion corresponding to each velocity deviation interval of TCMR (m/s) for microbialite and coquina.

P-deviation	**Microbialite**		**Coquina**	
	Aspect Ratio	Proportion	Aspect Ratio	Proportion
Above 500 m/s	0.19	23 %	0.22	13%
±500 m/s (or less)	0.12	77%	0.13	84%
Below −750 m/s	–	–	0.05	3%

Thus, as shown in Table 1, the aspect ratio that best describes the microbialite considering P-velocity positive deviations above 500 m/s is 0.19, corresponding to a proportion of 23% of the interval; for deviations of $500m/s$, we found an aspect ratio of 0.12 with a proportion of 77%; deviations of less than −750 m/s were not observed. In coquina, there is an aspect ratio of 0.22 corresponding to a proportion of 13% for deviations above 500 m/s; an aspect ratio of 0.13 with a proportion of 84% for deviations of $500m/s$; and an aspect ratio of 0.05 with a proportion of 3% for deviations less than −750 m/s.

According to Silva et al. (2020), the values best fitting these well logs (P-velocity and S-velocity), obtained iteratively, correspond to the curve that considers the most extreme points of the crossplots of the P-velocity deviation for microbialite and coquina, and not the curve that considered the midpoints (Table 2). Although discrepant, it is observed that: a) the highest frequency obtained for the aspect ratio values $\alpha_2 = 0.18$ represents velocity deviation values above 500 m/s (0.19), evidencing the predominance of vugs in the microbialite; and b) the velocity deviation of $500m/s$ for the coquina evidences the presence of vugs associated with intercrystalline and interparticle pores, which is an aspect ratio value (α_2=0.15) close to that showed in the Table 1 (0.13). Another point to be considered is the fact that in the modeling by Xu and Payne (2009), S-velocity also needs to be calibrated, in addition to P-velocity, and the aspect ratio values, as well as their frequency of occurrence, must be adequate for both seismic properties (P-velocity and S-velocity).

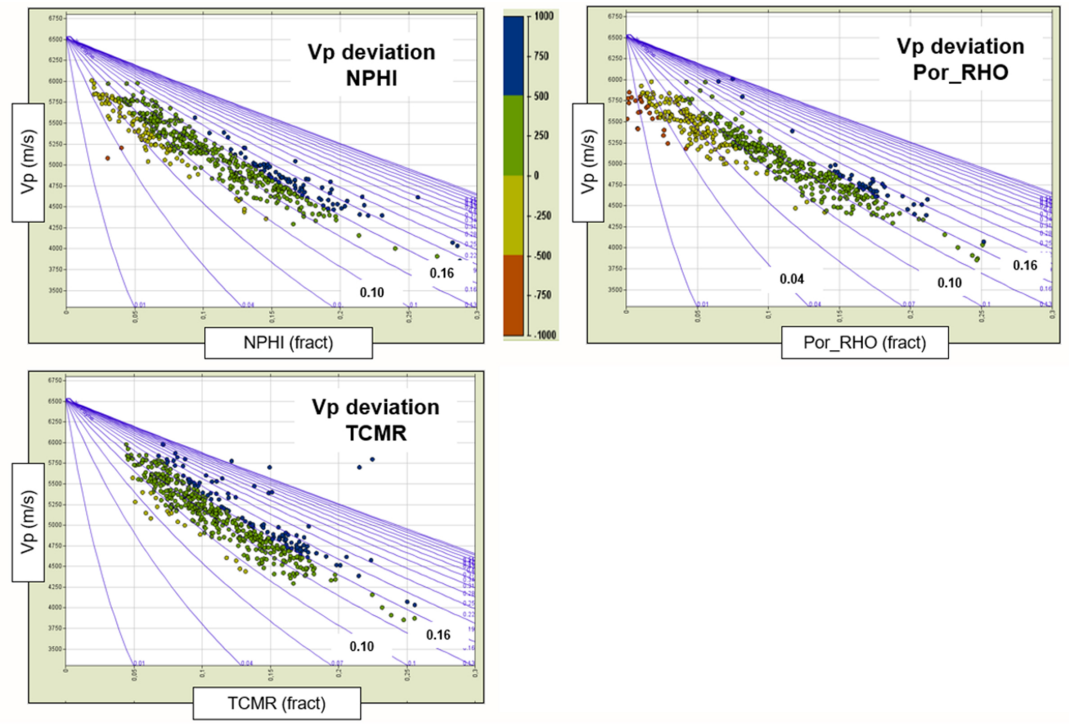

Figure 9: Porosity x P-velocity crossplot, colored by the velocity deviation of the P-wave (m/s) of the three porosities (NPHI, TCMR and Por_RHO) for the microbialite. The aspect ratio values are informed by the blue lines in the crossplot (variation between 0.01 and 0.5) in which the higher the value, the more rounded the pore. Deviations above 500 m/s are shown in blue; deviations below −500 m/s, in red; and deviations within 500 m/s were divided into green and yellow, to highlight positive and negative deviations, respectively.

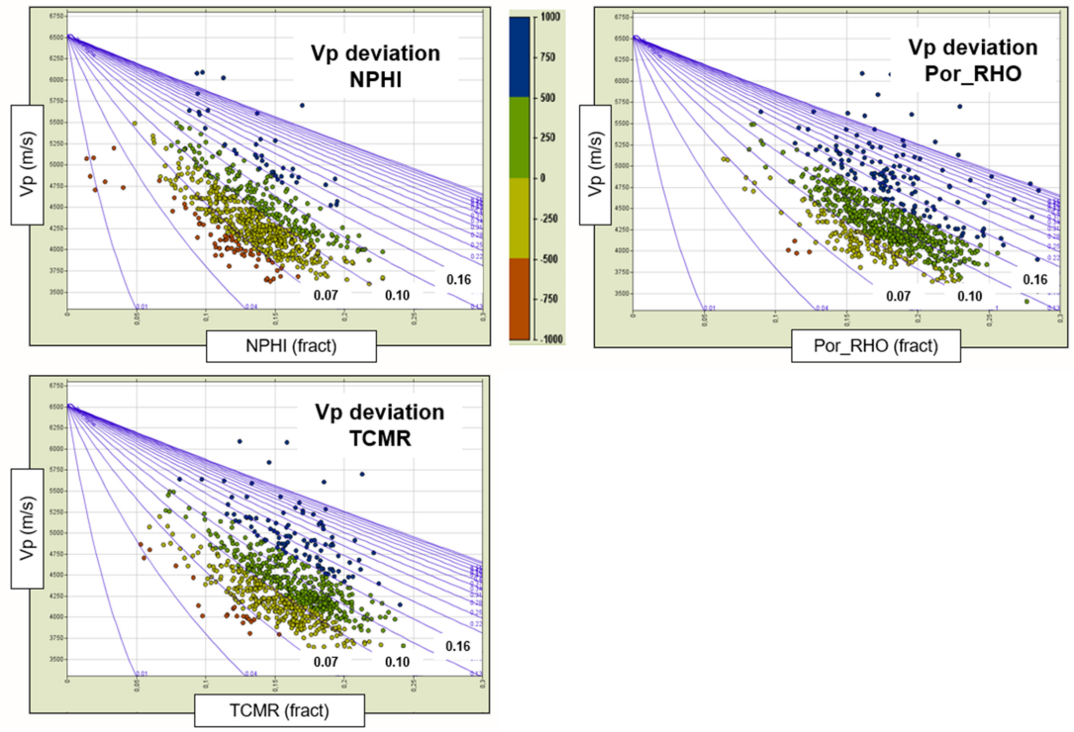

Figure 10: Porosity x P-velocity crossplot, colored by the velocity deviation of the P-wave (m/s) of the three porosities (NPHI, TCMR and Por_RHO) for the coquina. The aspect ratio values are informed by the blue lines in the crossplot (variation between 0.01 and 0.5) in which the higher the value, the more rounded the pore. Deviations above 500 m/s are shown in blue; deviations below −500 m/s, in red; and deviations within 500 m/s were divided into green and yellow, to highlight positive and negative deviations, respectively.

Table 2: Aspect ratio (α_1, α_2 and α_3) values and their respective frequency occurrences (F_1, F_2 and F_3) used in petroelastic modeling based on Xu and Payne (2009) for microbialite and coquina (Silva et al., 2020).

Aspect ratio for microbialite and coquina zones						
Zone	α_1	F_1 (%)	α_2	F_2 (%)	α_3	F_3 (%)
Microbialite	0.35	20	0.18	75	0.07	5
Coquina	0.35	20	0.15	75	0.04	5

CONCLUSION

We show that it is effective to use known patterns of velocity deviations in relation to pore types for predicting intervals of interest where there are no described samples.

Of the three velocity deviation curves analyzed, NPHI, TCMR and Por_RHO, the second was the one that best separated the microbialite facies from the coquina ones.

The vug pore is predominant in both intervals. In microbialite, it is more associated with intrafossil and moldic porosity and in coquina, it is mainly associated with moldic, interparticle and intercrystalline porosities.

Considering the differences in deviations from P-velocity, we state that the aspect ratios are representative of the same intervals for microbialite and coquina, showing very similar values.

The method is a good starting point to obtain aspect ratio values from P-velocity deviation prior to building petroelastic models to assist in seismic monitoring of the reservoir. However, some adjustments may be necessary, since the parameters must also fit in the calibration of S-velocity, in addition to P-velocity.

ACKNOWLEDGMENTS

This work was conducted with the support of Libra Consortium (Petrobras, Shell Brasil, Total Energies, CNOOC, CNPC), PPSA, and Energi Simulation through the ANP R&D levy fund for research and development. The authors are grateful for the support of the CEPETRO-UNICAMP/Brazil (Center for Petroleum Studies), the Department of Energy (DE-FEM-UNICAMP/Brazil) and UNISIM (Research in Reservoir Simulation and Management UNICAMP/Brazil). In addition, a special thanks to CMG, SLB, and CGG for the software licenses. The authors would also like to thank the Petrobras Reservoir Geophysics Management for their unlimited support of this work, especially Paulo Roberto Schroeder Johann and Rui Cesar Sansonowski, and the geophysicist Alexandre Rodrigo Maul for their consultancy. Finally, and most importantly, I thank God for the accomplishment of this work.

REFERENCES

Anselmetti, F. S., and G. P. Eberli, 1993, Controls on sonic velocity in carbonates: Pure and Applied Geophysics, **141**, 287–323, doi: 10.1007/BF00998333.

Anselmetti, F. S., and G. P. Eberli, 1997, Sonic velocity in carbonate sediments and rocks, *in* Carbonate Seismology: SEG Geophysical Developments Series, 4, 53–74. doi: 10.1190/1.9781560802099.ch4.

Anselmetti, F. S., and G. P. Eberli, 1999, The Velocity-Deviation Log: A tool to predict pore type permeability trends in carbonate drill holes from sonic and porosity or density logs: AAPG Bulletin, **83**, 450–466, doi: 10.1306/00AA9BCE-1730-11D7-8645000102C1865.

Castro, D. D., and P. L. F. Rocha, 2013, Quantitative parameters of pore types in carbonate rocks: Revista Brasileira de Geofísica, **31**, 125–136, doi: 10.22564/rbgf.v31i1.251.

Chang, H. K., R. O. Kowsmann, A. M. F. Figueiredo, and A. A. Bender, 1992, Tectonics and stratigraphy of the east Brazil rift system (EBRIS): an overview: Tectonophysics, **213**, 97–138, doi: 10.1016/0040-1951(92)90253-3.

Choquette, P. W., and L. C. Pray, 1970, Geologic nomenclature and classification of porosity in sedimentary carbonates: AAPG Bulletin, **54**, 207–250, doi: 10.1306/5D25C98B-16C1-11D7-8645000102C1865.

Faria, D. L., A. T. Reis, and O. G. Souza Jr., 2017, Three-dimensional stratigraphic sedimentological forward modeling of an aptian carbonate reservoir deposited during the sag stage in the Santos Basin, Brazil: Marine and Petroleum Geology, **88**, 676–695, doi: 10.1016/j.marpetgeo.2017.09.013.

Garcia, S. F. M., A. Danderfer Filho, D. F. Lamotte, and J.-L. Rudiewicz, 2012, Análise de volumes de sal em restauração estrutural: um exemplo na Bacia de Santos: Revista Brasileira de Geociências, **42**, 433–450, doi: 10.5327/Z0375-75362012000200016.

Harahap, R. F., A. Riyanto, and M. W. Haidar, 2020, Pore type-based carbonate reservoir characterization using rock physics modeling of "RF" field North Sumatera Basin: IOP Conference Series, The 4th Life and Environmental Sciences Academics Forum 2020, Indonesia, 012015. doi: 10.1088/1755-1315/846/1/012015.

Kukla, P. A., F. Strozyk, and W. U. Mohriak, 2018, South Atlantic salt basins witnesses of complex passive margin evolution: Gondwana Research, **53**, 41–57, doi: 10.1016/j.gr.2017.03.012.

Mann, J., and J. Rigg, 2012, New geological insights into the Santos Basin: GEOExPro, **9**, 36–40.

Maul, A., M. Cetale, C. Guizan, P. Corbett, J. R. Underhill, L. Teixeira, R. Pontes, and M. González, 2021, The impact of heterogeneous salt velocity models on the gross rock volume estimation: an example from the Santos Basin pre-salt, Brazil: Petroleum Geoscience, doi: 10.1144/petgeo2020-105.

Mavko, G., T. Mukerji, and J. Dvorkin, 2009, The rock physics handbook: tools for seismic analysis of porous media, 2nd ed.: Cambridge University Press. (doi: 10.1017/CBO9780511626753).

Moreira, J. L. P., C. V. Madeira, J. A. Gil, and M. A. P. Machado, 2007, Bacia de Santos: Boletim de Geociências da Petrobras, **15**, 531–549.

Ponte, F. C., and A. H. Asmus, 1978, Geological framework of the Brazilian continental margin: Geologische Rundschau, **67**, 201–235, doi: 10.1007/BF01803262.

Quirk, D. G., N. Schødt, B. Lassen, S. J. Ings, D. Hsu, K. K. Hirsch, and C. Von Nicolai, 2012, Salt tectonics on passive margins: examples from Santos, Campos and Kwanza basins, *in* Geological Society, London, Special Publications: **363**, 207–244. doi: 10.1144/SP363.10.

Saberi, R. M., 2013, Rock Physics Integration: From Petrophysics to Simulation: Presented at the 10th Biennial International Conference & Exposition, SPG, Kochi, Kerala, India. (Paper id: P444).

Silva, E. P. A., A. Davolio, M. S. Santos, and D. J. Schiozer, 2017, Application of velocity-deviation log to predict the aspect ratio in Pre-Salt Carbonate rocks: Presented at the 15th International Congress of the Brazilian Geophysical Society, SBGf, Rio de Janeiro, Brazil. doi: 10.1190/sbgf2017-183.

Silva, E. P. A., A. Davolio, M. S. Santos, and D. J. Schiozer, 2020, 4d petroelastic modeling based on a presalt well: Interpretation, **8**, T639–T649, doi: 10.1190/INT-2019-0099.1.

Wyllie, M. R. J., A. R. Gregory, and L. W. Gardner, 1956, Elastic wave velocities in heterogeneous and porous media: Geophysics, **21**, 41–70, doi: 10.1190/1.1438217.

Xu, S., and M. A. Payne, 2009, Modeling elastic properties in carbonate rocks: The Leading Edge, **28**, 66–74, doi: 10.1190/1.3064148.

Silva, E. P. A. da: Conceptualization (lead), writing (lead), review (lead) and editing (lead); **Davolio, A.:** Conceptualization (equal), writing (supporting), review (supporting) and editing (supporting); **Santos, M. S. dos:** Conceptualization (equal), writing (supporting), review (supporting) and editing (supporting); **Schiozer, D. J.:** Conceptualization (supporting), writing (supporting), review (supporting) and editing (supporting); **Santos, M. S. dos:** equal; **Schiozer, D. J.:** supporting.

Received on October 10, 2024 / Accepted on December 15, 2024